Microscopic Raman study of graphene on 4H-SiC two-dimensionally enhanced by surface roughness and gold nanoparticles

Hisatomo Matsumura[1], Shin-ichiro Yanagiya[1], Masao Nagase[2], Hiroki Kishikawa[1], and Nobuo Goto[1]

[1]*Department of Optical Science and Technology, Tokushima University, Tokushima 770-8506, Japan*

[2]*Department of Electrical and Electronic Engineering, Tokushima University, Tokushima 770-8506, Japan*

E-mail: syanagiya@tokushima-u.ac.jp

We present microscopic Raman spectroscopy measurements on single-layer graphene epitaxially grown on 4H-SiC by a thermal decomposition method. We collected spectral data with spatial resolution, which allowed us to obtain two-dimensionally enhanced Raman mapping images. Shallow holes in SiC, which had areas of 5 to 20 μm and depths of 100 nm, enhanced the Raman intensity of the 2D band of graphene. A monolayer of gold nanoparticle (AuNP) aggregates was successfully prepared by dropping and drying a colloidal suspension of AuNPs. The AuNP exhibited 30-fold enhanced the Raman spectra in the wavenumber range of 1550-1700 cm^{-1}. Locally enhanced Raman intensity was also demonstrated using a glass microbead.

1. Introduction

In this decade, graphene has attracted tremendous attention because of its novel electro-optic, photonic, and plasmonic properties[1-4]. Some graphene-based optical networking devices such as mode-locked fiber lasers[5-10], optical modulators[11-13], and optical switches[14-19] have been proposed, and some of these devices have practical applications. Most of the proposed devices have graphene integrated into an optical fiber or a planar waveguide[20]. To develop high-performance graphene-based devices, the growth and fabrication of high quality and large area graphene are necessary. Graphene is produced by exfoliation of highly ordered pyrolytic graphite (HOPG)[21], chemical vapor deposition[22], and thermal decomposition of SiC under vacuum or argon pressure. Nagase and co-authors reported the synthesis of large-area, high-quality epitaxial graphene on 4H-SiC by a thermal decomposition method, along with its resistivity anisotropy[23-25].

Here, gold nanoparticles (AuNPs) were deposited on large-area graphene/SiC. AuNPs are among the key materials in nanotechnology. They can enhance the Raman signals of neighboring materials, which is known as surface-enhanced Raman spectroscopy (SERS). Raman spectroscopy has been applied to the characterization of epitaxial graphene, graphene-based biosensors[26], and a switch architecture controlled by waveguide-type Raman amplifiers proposed by Kishikawa et al.[27] Large-area, high-quality SERS nanocomposites are necessary for the development of plasmonic devices employing Raman amplifiers, and gold–graphene nanocomposites were examined in the present study.

SERS effects of nanocomposites of AuNPs and graphene have been reported. Goncalves et al. reported the surface modification of graphene nanosheets with AuNPs[28]. Sekine et al. reported Ag-coated graphene/SiC synthesized by vapor deposition[29]. SERS depends on the size and shape of NPs; therefore, we studied size-controlled AuNPs. Size-

controlled AuNPs grow into two- or three-dimensional artificial opal[30]; Toyotama et al. reported that high-quality colloidal crystals of AuNPs can be grown by controlling the surface charge[31]. Highly ordered, self-assembled AuNPs hold promise as large-area, high-performance hybrid SERS materials.

In the present study, local Raman enhancement of graphene was studied by microscopic Raman spectroscopy. First, we demonstrated local Raman intensity differences resulting from the surface morphology of SiC. Following this, SERS effects caused by the local deposition of size-controlled AuNPs, which exhibit surface plasmon resonance (SPR) at the wavelength of the excitation laser (543 nm), were studied. In addition, a glass microbead (MB) was examined to emphasize the Raman intensity of graphene. The glass MB serves as a microlens[32] and enables whispering gallery modes (WGMs) for certain wavelengths and diameters. The combined effects of AuNP in shallow holes and a glass MB were also explored.

2. Experimental methods

A graphene sample was prepared by the thermal decomposition of 4H-SiC, as reported by Nagase and co-workers.[23-25] The sample was fabricated from a 4H-SiC(0001) substrate manufactured by Cree. The annealing condition was at 1750 °C under a pressure of 100 Torr in an argon atmosphere. Gold colloidal suspension was purchased from BBI Solutions (gold colloid, 60 nm). Figure 1 shows the absorption spectrum of the suspension, which had an absorption peak at 536 nm. The suspension was deposited on the surface of graphene and dried. Glass MBs, which were obtained from Polyscience (10-60 μm in diameter), were also deposited on the graphene surface. The sample was examined by microscopic Raman spectroscopy.

Raman spectra were obtained using a Raman spectrometer (Renishaw InVia Reflex). Measurements were performed at room temperature in air. The excitation laser had a wavelength of 532 nm and was focused using either a ×20 or ×50 objective lens. Raman mapping images were constructed from the Raman intensities of the G and 2D bands obtained using a ×100 objective lens. The resolution of the mapping was 21 pixels per 10 μm. The surface morphology of graphene/4H-SiC and the distribution of AuNP were observed using an atomic force microscope (AFM) and scanning electron microscope (SEM).

3. Results and discussion

First, the effect of the surface morphology of SiC on Raman intensity was studied. Figures 2(a) and 2(b) respectively show an optical microscope (OM) image of the graphene/4H-SiC surface with some regions of different optical contrast and the Raman spectra of graphene in the regions labeled B–E in (a). The Raman peaks of graphene at 1300–1400 cm^{-1} (D band), 1600 ± 50 cm^{-1} (G band), and 2700 ± 50 cm^{-1} (2D band) as well as of SiC (1500–1550 and 1700–2000 cm^{-1}) can be recognized in all Raman spectra.[29] The Raman intensity in these regions was almost the same and approximately 3–5 times higher than that in any other region of the surface. Figure 2(c) shows the microscopic Raman mapping image of the 2D band of graphene (2700 cm^{-1}). The regions observed with the OM correspond exactly to the areas where the Raman intensity is high. To identify the Raman-enhanced region, the surface morphology was observed with an AFM. Figures 2(d) and 2(e) show the height image and the height profile along the line indicated in the AFM image. The regions were shallow holes, 5 to 20 μm^2 in area and 100 nm in depth. The bottom of the holes had a roughness of ±20 nm. Zhao et al. have reported that the surface roughness of silver enhanced the Raman intensity of graphene[33]. The enhancing effect of SiC is weaker

than those of silver and gold, but the rough SiC surface at the bottom of the holes slightly enhanced the Raman intensity of graphene. Unfortunately, the cause of shallow hole generation is unknown. In our future study, the artificial micro-patterning of SiC before the growth of graphene should clarify the effect and graphene grown from micro-patterned SiC would be promising novel plasmonic devices.

The shallow holes on graphene/4H-SiC exhibited 3-5 times higher Raman intensity of SiC than the other regions, as shown in Fig. 2. Following this, the Raman spectra of AuNPs buried in the shallow holes were studied. Figure 3 shows an optical image, an SEM image, and Raman spectra of AuNPs on graphene/4H-SiC. AuNPs were buried in a hole and were 2-3 layers thick. The Raman spectra of graphene on the flat surface (point A), in the hole (point B), and in the hole with AuNPs (point C) are shown in Fig. 3(c). To quantify the Raman intensity of graphene, spectra A and B were normalized to fit the Raman spectra of SiC (1700–1900 cm^{-1}). The Raman intensities in the hole were twofold higher for G and D bands and fivefold higher for the 2D band than those on the flat surface. The Raman spectrum at point C changed its shape and became 30 times larger than that of graphene/SiC. Figure 3(d) shows multi-peak fitting of Raman spectrum of AuNP/graphene/SiC by the gaussian curves that have peaks at 1350, 1510 and 1590 cm^{-1}, which are identified as the D band of graphene, the highest peak of SiC, and the G band of graphene, respectively. The peak was successfully fitted by the Gaussian curves. This suggests that AuNPs enhance the spectrum of graphene/SiC.

Next, we further investigated the Raman spectrum of AuNPs deposited on the surface of graphene/4H-SiC (AuNP/graphene/4H-SiC). Figure 4 shows an OM image, an SEM image, and a Raman spectrum of AuNP/graphene/4H-SiC. The monolayer colloidal crystals of AuNPs, which were 60 nm in diameter, grew two dimensionally on a flat surface of

graphene/4H-SiC, as shown in Fig. 4(b). Larger colloidal crystals tended to have two or more layers. Figure 4(c) shows the Raman spectra of AuNP/graphene/SiC, AuNP/SiC, and AuNP/glass. The Raman spectrum of AuNP was ten times larger than that of graphene/SiC shown in Fig. 3(c) and had no peaks in the range of 1300-2900 cm^{-1}. On the other hand, the Raman spectrum of AuNP/graphene/SiC had a peak at 1300-1700 cm^{-1}. The Raman spectrum of AuNP/SiC had a similar peak but the wavenumber at the highest intensity was 1510 cm^{-1}, which was different from the 1590 cm^{-1} of AuNP/graphene/SiC. Note that the spectrum was broad and the peak at 1800 cm^{-1} of SiC disappeared. This suggests that AuNPs enhanced the spectrum of graphene/SiC as a result of not only SERS of AuNP but also more complicated photonic effects.

Following this, another combined enhancement using holes with a glass MB was demonstrated. Figure 5 shows an optical image and the corresponding microscopic Raman intensity mapping images for the graphene 2D band. The Raman intensity at the glass bead was higher than that at any other region in the image. The high intensity depended on the size of the glass bead, magnitude of the objective lenses, and focal plane and point. It can be seen from the Raman image that the high-intensity region was almost the same as the area of the glass MB when a relatively low magnification (×20) was used and the focal point was at the center of the MB. Figure 5(c) shows the spectra of MB/graphene/4H-SiC. When three Raman spectra were fit over the range from 1500 to 1900 cm^{-1}, the baseline of the Raman spectrum at point C was higher than those of the other spectra. This suggests that the MB, acting like a microlens, gathered light and assisted in the concentration of light at graphene.

In this study, Raman enhancement of graphene, which could be observed by optical microscopy, was demonstrated. Shallow holes in SiC not only enhanced the Raman signal of graphene D, G, and 2D bands but also accommodated AuNPs. The degrees of

enhancement were lower than those for AuNPs but this technique will be essential for the microfabrication of devices using hybrid materials containing graphene, AuNPs, and SiC. On the other hand, AuNPs enhanced the Raman signals of graphene/SiC to a particular range from 1500-1700 cm^{-1} by one order of magnitude. This suggests that the AuNP might cause enhancement not only by SERS (material selectivity) but also by other photonic effects (wavelength selectivity). In a previous paper, it was reported that a 10-nm-thick layer of silver NPs was deposited on the graphene/SiC by a dry process and had a hemispherical shape[28]. They (Ag/graphene/SiC) selectively enhanced the Raman signal of graphene. In contrast to the hemispherical Ag for which the contacting edge with graphene was visible, the contact point between the AuNP and graphene in this study was invisible because it was underneath the AuNPs. Therefore, the Raman spectrum was obtained through an indirect optical path and shows wavelength-selective enhanced Raman signals. Although globular AuNPs show complicated Raman enhancement, they have advantages in material fabrication. We can use size-controlled AuNPs that affects the surface plasmon polariton. Additionally, the size-controlled AuNPs can grow into colloidal crystals[30]. The photonic effects of the colloidal crystal of AuNP on graphene SiC will be investigated in a future study.

4. Conclusions

Raman enhancements of graphene/4H-SiC by surface modification, a gold nanoparticle (AuNP) film, and a glass microbead were proposed and demonstrated. Surface modification of shallow holes enhanced the Raman signals of the D, G, and 2D bands of graphene by 3–5 times compared with those of a flat surface. The monolayer of AuNPs 60 nm in diameter

exhibited 30-fold enhanced Raman spectra in the wavenumber range of 1550-1700 cm^{-1} of graphene/SiC. The glass microbead also locally enhanced the Raman intensity of graphene by gathering light from the surface of graphene/SiC.

Acknowledgments

This work was supported by the Japan Society for the Promotion of Science (JSPS) KAKENHI (Grant No. 15K04679 for S. Yanagiya and 26289107 for M. Nagase).

References

1) K. S. Novoselov, V. I. Fal'ko, L. Colombo, P. R. Gellert, M. G. Schwab, and K. Kim, Nature **490,** 192 (2012).
2) S. Yamashita, J. Lightwave Technol. **30,** 427 (2012).
3) F. Bonaccorso, Z. Sun, T. Hasan, and A. C. Ferrari, Nat. Photonics **4,** 611 (2010).
4) Q. L. Bao, H. Zhang, Y. Wang, Z. H. Ni, Y. L. Yan, Z. X. Shen, K. P. Loh, and D. Y. Tang, Adv. Funct. Mater. **19,** 3077 (2009).
5) D. Popa, Z. Sun, F. Torrisi, T. Hasan, F. Wang, and A. C. Ferrari, Appl. Phys. Lett. **97** (2010).
6) Y.-W. Song, S.-Y. Jang, W.-S. Han, and M.-K. Bae, Appl. Phys. Lett. **96** (2010).
7) H. Zhang, D. Y. Tang, L. M. Zhao, Q. L. Bao, and K. P. Loh, Opt. Express **17,** 17630 (2009).
8) H. Zhang, Q. Bao, D. Tang, L. Zhao, and K. Loh, Appl. Phys. Lett. **95** (2009).
9) H. Zhang, D. Tang, R. J. Knize, L. Zhao, Q. Bao, and K. P. Loh, Appl. Phys. Lett. **96** (2010).
10) Z. P. Sun, T. Hasan, F. Torrisi, D. Popa, G. Privitera, F. Q. Wang, F. Bonaccorso, D. M. Basko, and A. C. Ferrari, ACS Nano **4,** 803 (2010).
11) M. Liu, X. Yin, and X. Zhang, Nano Lett. **12,** 1482 (2012).
12) R. Hao, W. Du, H. Chen, X. Jin, L. Yang, and E. Li, Appl. Phys. Lett. **103** (2013).
13) E. O. Polat and C. Kocabas, Nano Lett. **13,** 5851 (2013).
14) H. Wang, H. Su, H. Qian, Z. Wang, X. Wang, and A. Xia, J. Phys. Chem. A **114,** 9130 (2010).
15) S. J. Koester, H. Li, and M. Li, Opt. Express **20,** 20330 (2012).
16) M. Oya, H. Kishikawa, N. Goto, and S. Yanagiya, Opt. Express **20,** 27322 (2012).
17) M. Takahashi, W. Ueda, N. Goto, and S. Yanagiya, IEEE Photonics J., **5,** 6602109 (2013).
18) T.-Z. Shen, S.-H. Hong, and J.-K. Song, Nautre Mater. **13,** 394 (2014).
19) M. Takahashi, H. Kishikawa, N. Goto, and S. Yanagiya, J. Lightwave Technol. **32,** 4226 (2014).
20) Q. L. Bao and K. P. Loh, ACS Nano **6,** 3677 (2012).
21) K. S. Novoselov, A. K. Geim, S. V. Morozov, D. Jiang, Y. Zhang, S. V. Dubonos, I. V. Grigorieva, and A. A. Firsov, SCIENCE **22**, 666 (2004).
22) X. Li, W. Cai, J. An, S. Kim, J. Nah, D. Yang, R. Piner, A. Velamakanni, I. Jung, E. Tutuc, S. K. Banerjee, L. Colombo, and R. S. Ruoff, Science **324** 1312 (2009)
23) O. Ryong-Sok, A. Iwamoto, Y. Nishi, Y. Funase, T. Yuasa, T. Tomita, M. Nagase, H. Hibino, and H. Yamaguchi, Japanese J. Appl. Phys. **51** (2012).
24) S. Tanabe, Y. Sekine, H. Kageshima, M. Nagase, and H. Hibino, Appl. Phys. Express, **3,** 075102, (2010).
25) K. Kobayashi, S. Tanabe, T. Tao, T. Okumura, T. Nakashima, T. Aritsuki, R.-S. O, and M. Nagase, Appl. Phys. Express **8**, 036602 (2015).
26) T.-H. Kim, K.-B. Lee, and J.-W. Choi, Biomaterials **34**, 8660 (2013).
27) H. Kishikawa, K. Kimiya, N. Goto, and S. Yanagiya, J. Lightwave Technol. **28,** 172 (2010).

28) G. Goncalves, P. A. A. P. Marques, C. M. Granadeiro, H. I. S. Nogueira, M. K. Singh, and J. Grácio, Chem. Mater., **21**, 4796 (2009).
29) Y. Sekine, H. Hibino, K. Oguri, T. Akazaki, H. Kageshima, M. Nagase, K. Sasaki, and H. Yamaguchi, NTT Tech. Rev. **11**, 1 (2013).
30) T. Ohkubo, *Utsukushii koroido to kaimen no sekai* (Matuo Shuppan, Tokyo, 2001) p. 150 [in Japanese]
31) A. Toyotama, M. Yamamoto, Y. Nakamura, C. Yamazaki, A. Tobinaga, Y. Ohashi, T. Okuzono, H. Ozaki, F. Uchida, and J. Yamanaka, Chem. Mater., **26**, 4058 (2014).
32) Y. Yan, Y. Zeng, Y. Wu, Y. Zhao, L. Ji, Y. Jiang, and L. Li, Opt. Express **22,** 23552 (2014).
33) Y. Zhao, X. Liu, D. Y. Lei, and Y. Chai, Nanoscale **6**, 1311 (2014).

Figure Captions

Fig. 1. UV-Vis spectrum of gold colloidal suspension consisting of 60-nm-diameter particles.

Fig. 2. (Color online) (a) Optical image of graphene/4H-SiC. The sample was illuminated by white light and observed using a ×50 objective lens. (b) Raman spectra of graphene/4H-SiC at the points indicated in (a). Lines b–e are offset from line a by 300 counts on the Y-axis. The peaks that represented in the figure were identified as D band (G:D, 1400 cm^{-1}), G band (G:G, 1590 cm^{-1}), and 2D band (G:2D, 2700 cm^{-1}) of graphene and SiC (1500 cm^{-1}, 1700-2000 cm^{-1}). (c) Raman mapping image of the 2D band of graphene in the same microscopic field as the optical image (a). (d) AFM image of the surface morphology of graphene/4H-SiC. (e) Height profile along the white line in (d).

Fig. 3. (Color online) (a) Optical image of AuNP/graphene/4H-SiC. (b) SEM image and (inset) Raman mapping image at 1600 cm^{-1}. (c) Raman spectra of the regions indicated in (b). The spectra of graphene on the flat surface (A) and in the hole (B) were normalized to fit the Raman peaks in the range of 1600–1800 cm^{-1}. The Raman intensity at point C is shown on the right axis. (d) Multiple peak fitting of (c) against the data in the range of 1350–1800 cm^{-1} by Gaussian curves that have peaks at 1350 (D band), 1510 (typical SiC), and 1590 cm^{-1} (G band).

Fig. 4. (Color online) (a) Optical image of AuNPs on graphene/4H-SiC. (b) SEM image of the AuNP island indicated by the white circle in (a). (c) Raman spectra of AuNP/graphene/4H-SiC, AuNP/SiC, and AuNP/glass. To compare the shapes of the peaks, the AuNP/SiC and AuNP/glass spectra were offset on the y-axis (18000 and 16000 arb. unit, respectively).

Fig. 5. (Color online) (a) Optical image and (b) corresponding Raman intensity mapping

image of 2D band of graphene at a glass MB on graphene/4H-SiC. A ×20 objective lens was used for the observation. (c) Raman spectra of the points shown in (b).

Figures

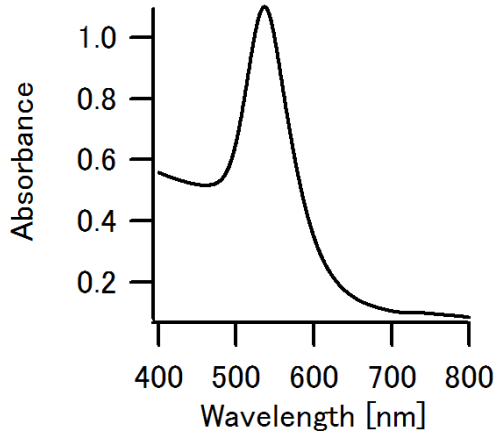

Figure 1

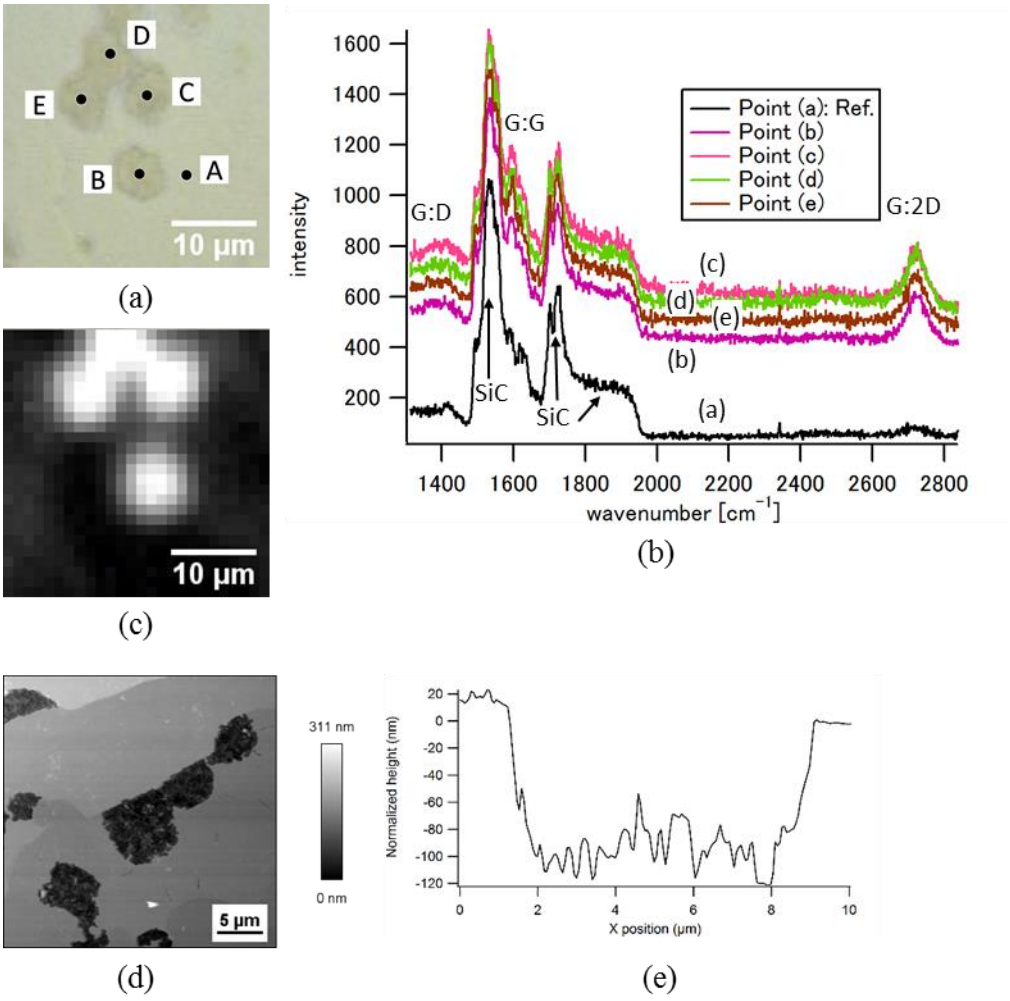

Figure 2 (Color online)

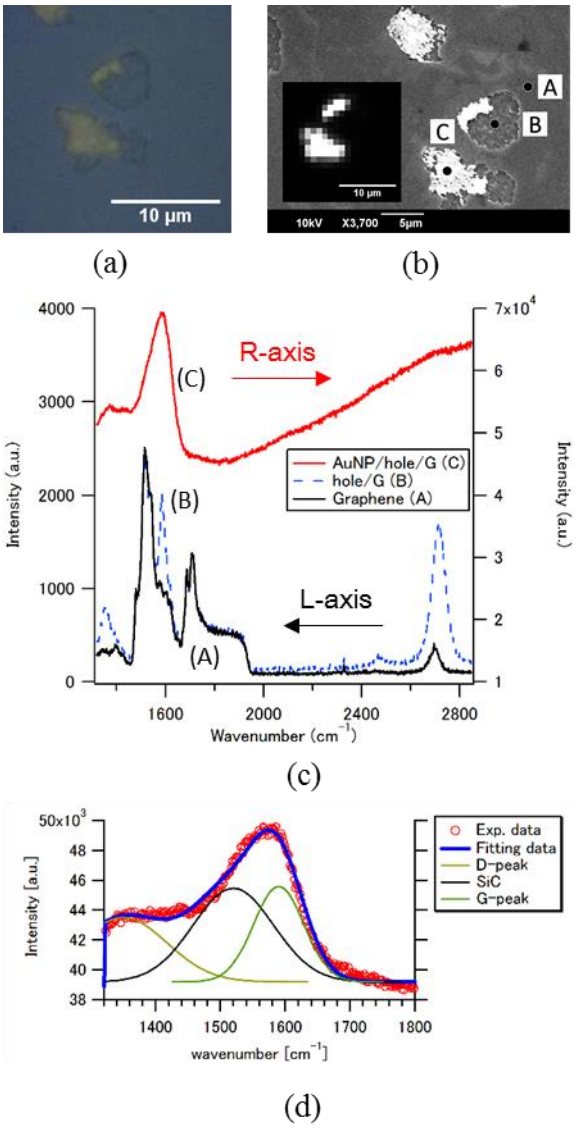

Figure 3 (Color online)

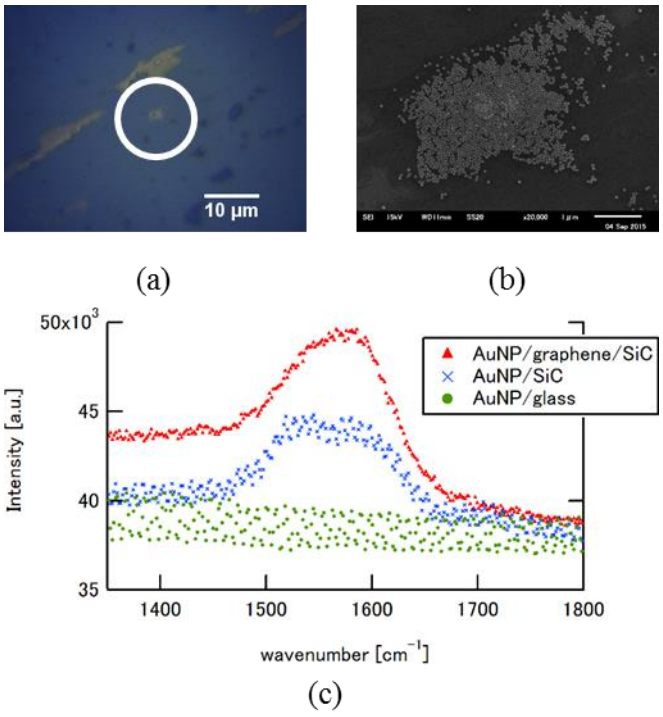

Figure 4 (Color online)

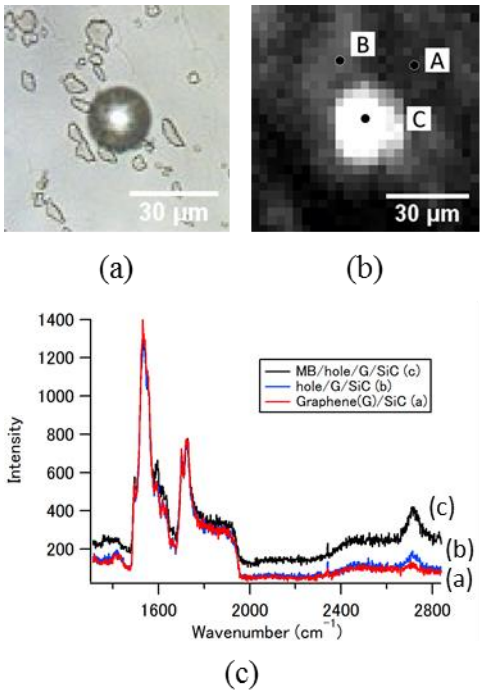

Figure 5 (Color online)